Analysis of Correlation-Aware Header Placement in LR-FHSS Under Unslotted ALOHA Access

Dengke Wang, *Member, IEEE*, Zhihong Zeng, *Member, IEEE*, Fengli Yang, *Member, IEEE*, Chen Chen, *Senior Member, IEEE*, Jia Ye, *Member, IEEE*, Harald Haas, *Fellow, IEEE*

***Abstract*—Long-Range Frequency Hopping Spread Spectrum (LR-FHSS) packets rely on repeated headers to enable synchronization and payload recovery, yet current designs place all header replicas at the packet front. Under unslotted ALOHA access, this creates strongly correlated header collisions because a single interferer can simultaneously overlap multiple adjacent headers. Existing LR-FHSS analyses usually neglect this effect by treating segment collisions as independent, which obscures the role of header placement in packet reliability. This letter develops a correlation-aware analytical framework that exploits the offset-dependent header-overlap structure together with multi-header inclusion–exclusion to capture the resulting correlation among header collision events. Closed-form collision probabilities are derived to quantify this correlation. Three representative header-placement principles, namely, clustered, split front/end, and separated placement, are then compared. Numerical results show that splitting the header replicas between the packet front and end decorrelates their collisions and lowers the packet loss rate (PLR) relative to the clustered design, under both the collision and partial-collision models; this decorrelation makes the simple independent-segment model accurate for the split layout while it underestimates the clustered one, providing a practical LR-FHSS design guideline.**

***Index Terms*—LR-FHSS, ALOHA, header placement, packet loss rate, IoT.**

I. Introduction

The explosive growth of Internet of Things (IoT) devices demands low-power wide-area technologies that can support massive connectivity over extended coverage areas. In direct-to-satellite (DtS) IoT scenarios, where terrestrial infrastructure is unavailable, Long-Range Frequency Hopping Spread Spectrum (LR-FHSS) has emerged as a promising physical layer because it combines frequency hopping and lightweight coding to improve robustness under long propagation delays and dense random access [1]–[3].

Recent research has substantially expanded the LR-FHSS design space beyond baseline performance evaluation. Waveform and receiver enhancements, such as wide-gap hopping sequences and demodulator allocation, have been shown to improve decoding scalability [4]. Coding-oriented studies have strengthened header and payload robustness through network-coded header combinations [5] and segment-level erasure recovery [6]. Message-level transmission policies have also been investigated for dense LR-FHSS deployments [7]. These works show that LR-FHSS can be improved along several complementary directions. At the physical layer, LR-FHSS divides the operating channel width (OCW) into narrow $488\,\text{Hz}$ occupied-bandwidth (OBW) subchannels arranged in grids, and each header or payload segment hops within a single grid, giving $N = 35$ subchannels for the $137\,\text{kHz}$ OCW and $N = 86$ for the $336\,\text{kHz}$ OCW [3]. A related design instead partitions the grid's channels into disjoint subsets for the headers and the payload, reducing collisions at light load [10]. At the gateway, a sliding-window receiver detects a header by preamble correlation and, from a single decoded replica, regenerates the hop pattern to locate the remaining replicas and payload fragments [9].

However, [5], [6] also indicate that header transmission remains a critical reliability bottleneck. One structural aspect has received far less attention: the placement of replicated headers within an LR-FHSS packet. Since the receiver must decode at least one header before processing the coded payload fragments, simultaneous loss of all header replicas causes packet failure. Yet the current LoRaWAN design clusters all header replicas at the packet front [3], making them vulnerable to a single asynchronous interferer that overlaps several adjacent headers at once. Existing analyses often rely on the independent-segment model [3], [6], [8], which is tractable but cannot capture how header timing affects the probability that all replicas are lost together. Therefore, to the best of our knowledge, a correlation-aware packet loss rate (PLR) analysis for arbitrary header placement is still missing.

This letter addresses that gap by quantifying how header placement affects LR-FHSS PLR. The main contributions are twofold. (1) On the analysis side, we develop a correlation-aware PLR framework for arbitrary header placement by combining offset-dependent overlap characterization, multi-header inclusion–exclusion, and closed-form collision probabilities, thereby capturing simultaneous collisions among replicated headers. (2) On the design side, we use this framework to compare practical header-placement principles and show that temporal header separation reduces correlated header losses without additional coding or protocol overhead.

This work was supported in part by the National Natural Science Foundation of China under Grant 62271091 and 62501088, and in part by the Fundamental Research Funds for the Central Universities under Grant 2024CDJXY020. (Corresponding authors: Dengke Wang; Chen Chen.)

D. Wang, Z. Zeng, F. Yang, and C. Chen are with School of Microelectronics and Communication Engineering, Chongqing University, Chongqing 400044, China (email: dengke.wang@cqu.edu.cn; zhihong.zeng@cqu.edu.cn; cqu_yfl@cqu.edu.cn; and c.chen@cqu.edu.cn).

J. Ye is with State Key Laboratory of Power Transmission Equipment Technology, School of Electrical Engineering, Chongqing University, Chongqing 400044, China (e-mail: 20241101050@stu.cqu.edu.cn and j.ye@cqu.edu.cn).

Harald Haas is with Department of Engineering, University of Cambridge, 9 JJ Thomson Avenue, Cambridge CB3 0FA, UK (e-mail: huh21@cam.ac.uk).

II. SYSTEM MODEL

We consider the LR-FHSS uplink, in which a packet is transmitted as a sequence of frequency-hopped bursts over a narrowband channel partitioned into multiple hopping subchannels [3]. Under unslotted ALOHA access, both header and payload bursts are exposed to asynchronous collisions across time and frequency. This section first introduces the LR-FHSS packet structure, then presents the interference and decoding model, and finally describes the considered header-placement principles.

A. Packet Structure

We follow the standard LR-FHSS burst format and model a tagged packet as a sequence of K_h header replicas and M payload segments, where the repeated headers convey the information needed for payload decoding and hopping-sequence reconstruction [3]. The payload is carried by coded fragments, so successful decoding only requires that a sufficient number of fragments survive. Each header has duration τ_h and each payload segment has duration τ_p. The total packet duration is $T = K_h\tau_h + M\tau_p$. The packet is described by a segment-length vector $\boldsymbol{\ell} = [\ell_1, \ell_2, \ldots, \ell_{K_h+M}]$, where each entry is either τ_h for a header replica or τ_p for a payload fragment. The start and end times of segment i are

$$s_i = \sum_{k=1}^{i-1} \ell_k, \quad e_i = s_i + \ell_i. \tag{1}$$

During transmission, each segment occupies one hopping interval and independently hops to one of the N available subchannels with equal probability.

B. Interference and Decoding Model

The system is assumed to follow an ALOHA-type random access protocol, consistent with LoRaWAN operation. Accordingly, I interfering packets arrive with random time offsets $\Delta_k \sim \mathrm{Unif}[-T, T]$, $k = 1, \ldots, I$, independently. The interval $[-T, T]$ contains all relative offsets that can produce a nonzero overlap with the tagged packet; offsets outside this range cannot affect reception and therefore do not contribute to the PLR. Each interferer has the same segment structure as the tagged packet and independently hops over the available subchannels. Segment i of the tagged packet is collided by segment j of an interferer at offset Δ if $s_i < \Delta + e_j$ and $e_i > \Delta + s_j$, and both segments occupy the same subchannel. A collided segment is assumed to be lost and therefore cannot contribute to header or payload decoding. Let $\mathcal{L}_{h,u}$ and $\mathcal{L}_{p,i}$ denote the loss events of header replica u and payload segment i, respectively, where $u = 1, \ldots, K_h$ and $i = 1, \ldots, M$. The superscript c denotes the complement event, so $\mathcal{L}_{h,u}^c$ and $\mathcal{L}_{p,i}^c$ represent successful reception of the corresponding header and payload segments.

Let $\mathcal{H}$ and $\mathcal{P}$ denote the header- and payload-success events, respectively. The header is successfully received if at least one of the K_h header replicas survives, i.e., $\mathcal{H} = \bigcup_{u=1}^{K_h} \mathcal{L}_{h,u}^c$. The payload is successfully received if at least m_0 out of the M payload segments survive, where m_0 is the minimum number of unerased coded segments required by the payload code:

$$\mathcal{P} = \left\{ \sum_{i=1}^{M} \mathbf{1}\{\mathcal{L}_{p,i}^c\} \geq m_0 \right\}. \tag{2}$$

Accordingly, a packet is successfully decoded if both $\mathcal{H}$ and $\mathcal{P}$ occur. The PLR is given by $\mathrm{PLR} = 1 - \mathrm{P}(\mathcal{H} \cap \mathcal{P})$.

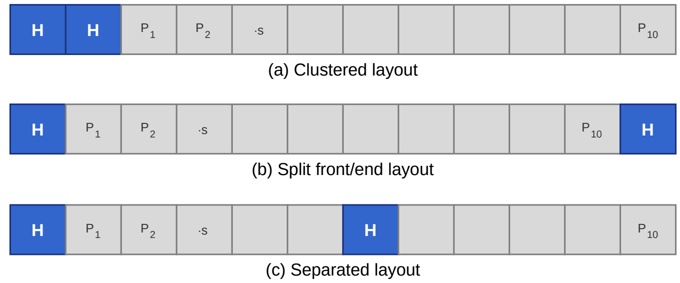

Fig. 1. Representative header-placement principles. Each segment (header or payload) is transmitted on a randomly selected subchannel.

C. Header Placement Strategies

Because the sliding-window receiver [9] recovers a packet irrespective of its position, we therefore consider three representative placement principles (Fig. 1 illustrates the case $K_h = 2$). The first is the clustered layout, in which all headers are placed at the beginning, followed by the M payload segments. The second is the split front/end layout, in which one header is kept at the beginning while the remaining $K_h - 1$ replicas are moved to the end of the packet, after all payload segments. The third is a separated layout, in which the headers are distributed among payload segments rather than grouped together. Let $M_{\mathrm{L}} = \lfloor M/2 \rfloor$ and $M_{\mathrm{R}} = M - M_{\mathrm{L}}$. For $K_h = 2$, this gives $[H, P_1, \ldots, P_{M_{\mathrm{L}}}, H, P_{M_{\mathrm{L}}+1}, \ldots, P_M]$, whereas for $K_h = 3$, the corresponding arrangement is $[H, P_1, \ldots, P_{M_{\mathrm{L}}}, H, P_{M_{\mathrm{L}}+1}, \ldots, P_M, H]$.

III. PERFORMANCE ANALYSIS

Following the analytical treatment commonly adopted in prior LR-FHSS studies [5], [8], we approximate the packet success probability by decoupling the aggregate header-success event $\mathcal{H}$ from the aggregate payload-success event $\mathcal{P}$. Accordingly,

$$\mathrm{P}(\mathcal{H} \cap \mathcal{P}) \approx \mathrm{P}(\mathcal{H})\,\mathrm{P}(\mathcal{P}). \tag{3}$$

Under this approximation, the analysis is decomposed into two parts: the probability that the headers are not all lost, and the probability that sufficiently many payload segments survive. The key difficulty lies in the header term, because the collision events of different header replicas are correlated through the common interferer offset. The derivation below therefore begins by characterizing the offset-dependent overlap structure, then evaluates the joint no-collision probability for arbitrary header subsets, and finally extends the result to multiple interferers and to the payload-success event.

A. Header Success Framework

Let Δ denote the relative time offset between the tagged packet and a single interferer. For a given offset Δ, define the overlap set of header u as $\mathcal{A}_u(\Delta) = \{j : s_{h_u} < \Delta + e_j \text{ and } e_{h_u} > \Delta + s_j\}$, where h_u is the segment index of header u. The only role of Δ in the collision probability is to determine these overlap sets. As Δ varies, they change only at the transition points

$$\mathcal{B} = \bigcup_{u=1}^{K_h} \bigcup_{j=1}^{K_h+M} \{e_{h_u} - s_j,\ s_{h_u} - e_j\} \cap [-T, T]. \tag{4}$$

Let the ordered elements of $\mathcal{B} \cup \{-T, T\}$ be $b_0 < b_1 < \cdots < b_R$. The calculation has two levels. First, for a fixed interferer offset Δ, $g_{\mathcal{S}}(\Delta)$ gives the probability that this interferer does not collide with any header in the subset $\mathcal{S}$. Second, because asynchronous ALOHA access makes Δ random over $[-T, T]$, this fixed-offset quantity must be averaged over all possible offsets before it can be used in the header-loss probability. Between two consecutive points, every overlap set is fixed, so this offset average is evaluated by

$$\mathbb{E}_\Delta[g_{\mathcal{S}}(\Delta)] = \frac{1}{2T} \sum_{r=0}^{R-1} (b_{r+1} - b_r)\, g_{\mathcal{S}}\!\left(\tfrac{b_r + b_{r+1}}{2}\right). \tag{5}$$

For a single header, $\mathcal{S} = \{u\}$ and $g_{\{u\}}(\Delta) = (1 - 1/N)^{|\mathcal{A}_u(\Delta)|}$, since each overlapping interferer segment avoids the header subchannel with probability $1 - 1/N$. Let $p_{h,u}$ denote the probability that header u is safe from all I interferers. Applying (5) to $g_{\{u\}}(\Delta)$ and using the independence of the I interferers gives

$$p_{h,u} = \left(\mathbb{E}_\Delta \left[\left(1 - \frac{1}{N}\right)^{|\mathcal{A}_u(\Delta)|} \right] \right)^I. \tag{6}$$

The same construction extends directly to any nonempty header subset $\mathcal{S} \subseteq \{1, \ldots, K_h\}$. Let $p_{h,\mathcal{S}}$ be the probability that all headers in $\mathcal{S}$ are safe from all I interferers. After the fixed-offset function $g_{\mathcal{S}}(\Delta)$ is specified, (5) converts it into the average no-collision probability for one random interferer; independence across the I interferers then gives

$$p_{h,\mathcal{S}} = \left(\mathbb{E}_\Delta[g_{\mathcal{S}}(\Delta)]\right)^I. \tag{7}$$

These subset survival probabilities are then combined through inclusion–exclusion to obtain the probability that all headers are lost:

$$\mathrm{P}(\mathcal{H}^c) = 1 + \sum_{\emptyset \neq \mathcal{S} \subseteq \{1,\ldots,K_h\}} (-1)^{|\mathcal{S}|} p_{h,\mathcal{S}}. \tag{8}$$

The remaining task is to specify $g_{\mathcal{S}}(\Delta)$ for the header subsets required by (8). In other words, (5) provides the offset-averaging step, while the following expressions provide the subset-specific no-collision functions. For example, the inclusion–exclusion expansion for three headers uses the single-header terms $g_{\{u\}}$, the pair terms $g_{\{u,v\}}$, and the triple term $g_{\{1,2,3\}}$. A unified viewpoint is to classify each interferer segment according to which headers in $\mathcal{S}$ it overlaps, and then condition on the subchannel assignment pattern of these headers. Since LR-FHSS uses only two or three header replicas (more headers shift the bottleneck to the payload [6]), we evaluate the closed-form cases $|\mathcal{S}| = 2$ and $|\mathcal{S}| = 3$.

For $|\mathcal{S}| = 2$, let $a = |\mathcal{A}_1(\Delta)|$, $b = |\mathcal{A}_2(\Delta)|$, and $c = |\mathcal{A}_1(\Delta) \cap \mathcal{A}_2(\Delta)|$ denote the overlap counts with a single interferer, and define $q_k = 1 - k/N$. These counts depend on the offset Δ; this dependence is omitted on the right-hand side of the following expression for compactness. Conditioning on whether the two headers use the same subchannel (probability $1/N$) or different subchannels $(1 - 1/N)$, one obtains

$$g_{\{1,2\}}(\Delta) = \frac{1}{N} q_1^{a+b-c} + q_1^{a+b-2c+1} q_2^c. \tag{9}$$

The first term corresponds to $f_1 = f_2$: the c shared interferer segments need only avoid one frequency, while the remaining $a+b-c$ segments each avoid one frequency. The second term corresponds to $f_1 \neq f_2$: the c shared segments must avoid two distinct frequencies.

For $|\mathcal{S}| = 3$, the same principle is used, but the overlap pattern is richer. Each interferer segment j is categorized according to which of the three headers it overlaps, yielding offset-dependent counts $n_1(\Delta), n_2(\Delta), n_3(\Delta)$, $n_{12}(\Delta), n_{13}(\Delta), n_{23}(\Delta)$, and $n_{123}(\Delta)$. For example, define

$$\chi_{u,j}(\Delta) = \mathbf{1}\{[s_j + \Delta, e_j + \Delta] \cap [s_{h_u}, e_{h_u}] \neq \emptyset\}. \tag{10}$$

$$n_{12}(\Delta) = \sum_j \chi_{1,j}(\Delta)\chi_{2,j}(\Delta)\left(1 - \chi_{3,j}(\Delta)\right), \tag{11}$$

which counts the interferer segments that overlap headers 1 and 2 but not header 3. To keep the notation concise, the argument Δ is omitted below. Let $n_U = n_1 + n_2 + n_3 + n_{12} + n_{13} + n_{23} + n_{123}$. Let P_A, P_B, and P_C denote the conditional no-collision probabilities for the cases where the three headers use the same subchannel, exactly two equal subchannels, and three distinct subchannels, respectively. For the first case, $P_A = q_1^{n_U}$. For the second case, let Φ_{uv} denote the conditional no-collision probability for the equality pattern $f_u = f_v$. Since the three equality patterns are symmetric,

$$P_B = \tfrac{1}{3}\left(\Phi_{12} + \Phi_{13} + \Phi_{23}\right), \tag{12}$$

where the pair subscript is unordered, e.g., $n_{xz} = n_{\min(x,z),\max(x,z)}$, and

$$\begin{aligned} \Phi_{xy} &= q_1^{n_x+n_y+n_{xy}+n_z} q_2^{n_{xz}+n_{yz}+n_{123}}, \\ &\{x, y, z\} = \{1, 2, 3\}. \end{aligned} \tag{13}$$

For the third case,

$$P_C = q_1^{n_1+n_2+n_3}\, q_2^{n_{12}+n_{13}+n_{23}}\, q_3^{n_{123}}. \tag{14}$$

Combining the three conditional cases in (12)–(14) gives the triple-header no-collision function

$$g_{\{1,2,3\}}(\Delta) = \frac{P_A + 3(N-1)P_B + (N-1)(N-2)P_C}{N^2}. \tag{15}$$

This expression specifies $g_{\mathcal{S}}(\Delta)$ for the particular subset $\mathcal{S} = \{1, 2, 3\}$; substituting it into (5) then yields its offset-averaged no-collision probability.

B. Payload Success Probability

Once the header term has been characterized, the payload contribution is evaluated through the number of surviving coded fragments. Let p_s denote the average survival probability of a payload segment, obtained by averaging over all M payload positions:

$$p_s = \left(\frac{1}{M} \sum_{i=1}^{M} \mathbb{E}_\Delta \left[\left(1 - \frac{1}{N}\right)^{|\mathcal{A}_{p_i}(\Delta)|} \right] \right)^I, \tag{16}$$

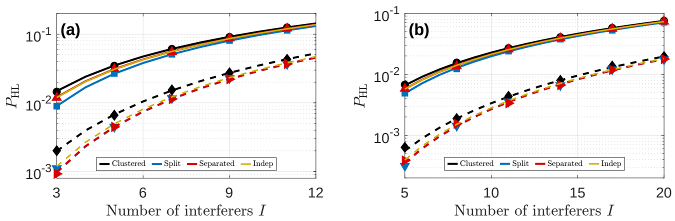

Fig. 2. Header loss probability $P_{\rm HL}$ versus number of interferers I, where solid and dashed lines correspond to $K_h = 2$ and $K_h = 3$, respectively. (a) $N = 35$; (b) $N = 86$.

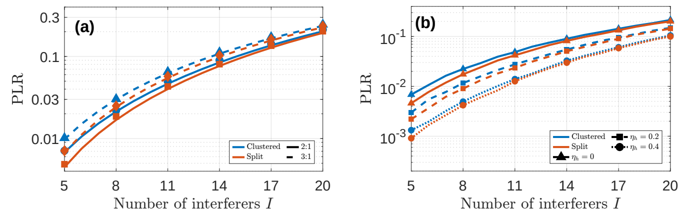

Fig. 3. PLR vs. interferers I. (a) Collision model ($\eta_h = 0$) under different header-to-payload ratios; (b) partial-collision model with different thresholds.

where $\mathcal{A}_{p_i}(\Delta)$ is the overlap set of the i-th payload segment. The averaging accounts for the fact that payload positions may experience different overlap statistics under different header placements. With the payload code requiring at least m_0 surviving fragments, the payload-success probability is then obtained by

$$\mathrm{P}(\mathcal{P}) = \sum_{r=m_0}^{M} \binom{M}{r} p_s^r (1-p_s)^{M-r}. \tag{17}$$

IV. Numerical Results

Unless otherwise stated, the numerical results use the following baseline parameters. The normalized segment durations are set to $\tau_h : \tau_p = 2$, close to the ratio of the LR-FHSS mode [3]. The default number of payload segments is $M = 10$, and the decoding threshold is set to $m_0 = \lceil M/3 \rceil$ [6]. The subchannel budget is set to $N = 35$, while the number of header replicas is taken as $K_h = 3$. Monte Carlo simulations use at least 10^5 trials per configuration. Curves represent analytical results, and markers represent Monte Carlo simulations.

Fig. 2 shows the probability $P_{\rm HL}$ that all header replicas are simultaneously lost, as a function of the number of interferers I. The split layout always yields the lowest $P_{\rm HL}$ under different subchannel budget N. For $K_h = 3$ the separated layout almost coincides with split, and the independent-segment baseline (yellow) lies just above both; for $K_h = 2$ the separated layout instead tracks the independent baseline, while only split stays below it. As the independent baseline ignores correlation, this shows that temporally spreading the replicas decorrelates their collisions: the clustered layout, whose adjacent replicas are positively correlated, sits above the baseline, so for the spread layouts the simpler independent model already suffices. The clustered–split gap is largest at the lighter loads shown and narrows as I grows, with all curves rising toward saturation, because heavy traffic eventually hits every header regardless of placement. The close agreement between analysis and simulation confirms the proposed expressions.

The PLR performance is summarized in Fig. 3, where the separated layout is omitted because Fig. 2 shows that it stays close to the split front/end layout. Fig. 3(a) reports the PLR under the collision model; the split front/end layout consistently lowers the PLR, and the gain grows with the header-to-payload ratio. Since each header is protected by a rate-$1/2$ convolutional code [3] and can therefore survive partial co-channel interference rather than being lost outright, Fig. 3(b) revisits the clustered-versus-split comparison under a partial-collision model, in which a header is declared lost only when the fraction of its duration collided by co-channel interference exceeds a tolerance η_h; the case $\eta_h = 0$ recovers the collision model of Fig. 3(a). As η_h increases from 0 to 0.4, the PLR of both layouts decreases, because a coded header then survives larger partial overlaps. Crucially, at every threshold the split layout stays at or below the clustered one, confirming that the header-placement gain persists under this more refined, partial-collision model.

V. Conclusion

This letter developed a correlation-aware PLR analysis for LR-FHSS with arbitrary header placement by combining offset-dependent overlap characterization, inclusion–exclusion, and closed-form no-collision probabilities. The results show that splitting the header replicas between the packet front and end weakens their collision correlation and lowers the PLR relative to the clustered layout under both the collision and partial-collision models; this decorrelation makes the simple independent-segment model accurate for the split layout while it underestimates the clustered one. The framework can be extended to more general traffic models and joint header-payload resource design.

References

[1] 3GPP, "Study on solutions for NR to support non-terrestrial networks (NTN)," TR 38.811, Release 15, 2020.

[2] Semtech Corporation, "LR-FHSS: Long Range–Frequency Hopping Spread Spectrum," LoRa Developer Portal, 2021.

[3] G. Boquet, P. Tuset-Peiró, F. Adelantado, T. Watteyne, and X. Vilajosana, "LR-FHSS: Overview and performance analysis," *IEEE Commun. Mag.*, vol. 59, no. 3, pp. 30–36, Mar. 2021.

[4] D. Maldonado, M. Kaneko, J. Fraire, A. Guitton, and O. Iova, "Enhancing LR-FHSS scalability through advanced sequence design and demodulator allocation," *IEEE Trans. Green Commun. Netw.*, early access, 2025.

[5] D. N. Knop, J. L. Rebelatto, and R. D. Souza, "LR-FHSS with network-coded header replication," *IEEE Trans. Veh. Technol.*, vol. 73, no. 6, pp. 9066–9070, Jun. 2024.

[6] D. Wang, A. Elzanaty, and M.-S. Alouini, "Coded frequency hopping for direct-to-satellite IoT systems: Design and analysis," *IEEE Internet Things J.*, vol. 11, no. 18, pp. 30206–30221, Sep. 2024.

[7] L. B. Rocha, J. M. S. Sant'Ana, M. A. Ullah, S. Montejo-Sánchez, J. L. Rebelatto, and R. D. Souza, "Toward improving the scalability of LR-FHSS: Transmission policies and performance analysis," *IEEE Open J. Commun. Soc.*, vol. 6, pp. 7075–7090, 2025.

[8] M. A. Ullah, K. Mikhaylov, and H. Alves, "Analysis and simulation of LoRaWAN LR-FHSS for direct-to-satellite scenario," *IEEE Wireless Commun. Lett.*, vol. 11, no. 3, pp. 548–552, Mar. 2022.

[9] J. M. de Souza Sant'Ana, O. da Silva Neto, A. Hoeller Jr., J. L. Rebelatto, R. D. Souza, and H. Alves, "Asynchronous contention resolution-aided ALOHA in LR-FHSS networks," *IEEE Internet Things J.*, vol. 11, no. 9, pp. 16684–16692, May 2024.

[10] J. M. de Souza Sant'Ana, E. J. dos Santos Jr., J. L. Rebelatto, K. Mikhaylov, H. Alves, and R. D. Souza, "LR-FHSS networks with orthogonal physical channels for headers and payload fragments," *IEEE Internet Things J.*, vol. 12, no. 16, pp. 34611–34614, 2025.